HIDDEN THIN LAYERS OF TOXIC DIATOMS IN A COASTAL BAY

A THESIS SUBMITTED TO THE GRADUATE DIVISION OF THE UNIVERSITY OF HAWAI'I AT MĀNOA IN PARTIAL FULFILLMENT OF THE REQUIREMENTS FOR THE DEGREE OF

MASTER OF SCIENCE

IN

OCEANOGRAPHY

AUGUST 2012

By

Amanda HV Timmerman

Thesis Committee:
Margaret McManus, Chairperson
Kathleen Ruttenberg
Karen Selph

ACKNOWLEDGEMENTS

I would like to thank my advisors, Margaret McManus and K. Ruttenberg, for their guidance and support; my other M.S. committee member K. Selph for her feedback; O. Cheriton, R. Cowen, A. Greer, R. Kudela and J. Sevadjian for their edits and assistance; D. Hull and R. Briggs for their assistance with laboratory analyses; A. McGaraghan for her help in the field and performing phytoplankton counts; D. McGehee and J. Warren for their discussions on acoustics; J. Ryan for his help with figures; C. Benitez-Nelson for her insight on *Pseudo-nitzschia* flocs; R. Bidigare for his help with laboratory methods; R. Moniz for providing tide data; Captains A. Macleod, A. Reynaga, J. Christman, J. Douglas for their technical assistance; G. Steward for his statistics assistance; K. Krogslund for her nutrient help; two reviewers for their helpful comments. The research described here is based upon work supported by the National Science Foundation Graduate Research Fellowship under Grant No. DGE-0822443 (A.H.V.T.), National Science Foundation Research Grant No. OCE-0925916 Lateral Mixing (M.A.M.) and National Science Foundation RAPID Grant No. OCE-1035047 (R.K.C.).

ABSTRACT

Harmful algal blooms (HABs) can threaten animal and human health through the production of toxins such as domoic acid. These blooms have become more frequent and toxic over the last few decades. In this study, we investigate the role that nutrients play in a toxic, subsurface bloom of *Pseudo-nitzschia* in northeastern Monterey Bay, California. Profilers and towed instruments were deployed and laboratory analyses of discrete water samples were conducted to describe the physical and biogeochemical conditions of the sampling site and to characterize the bloom. The *Pseudo-nitzschia* bloom occurred within a well-defined subsurface layer, containing high levels of domoic acid. *In situ* images taken within the layer revealed diatom flocs - indicators of nutrient stress. Nutrient ratios and alkaline phosphatase activity, commonly used to determine the nutritional status of phytoplankton, suggest that the *Pseudo-nitzschia* cells were phosphate stressed, and we speculate that this physiological stress led to increased toxicity of the bloom. Understanding how frequently blooms such as these are characterized by nutrient stress could improve our ability to predict the occurrence of HABs. With increased anthropogenic input of nutrients, such blooms could occur more often and with greater degrees of toxicity in the future.

TABLE OF CONTENTS

LIST OF TABLES

LIST OF FIGURES

1. INTRODUCTION

Harmful algal blooms (HABs) are a proliferation of photosynthetic organisms that have detrimental ecological and environmental impacts (Glibert et al., 2005). HABs may threaten animal and human health through the production of toxins such as domoic acid (DA) (Marchetti et al., 2004; Backer and McGillicuddy, 2006; Lefebvre and Robertson, 2010). Domoic acid is a neuroexcitatory amino acid (Buck et al., 1992), and species of the diatom genus *Pseudo-nitzschia* are among a number of organisms capable of producing it (Subba Rao et al., 1988; Bates et al., 1989; Mos, 2001; Lefebvre and Robertson, 2010). DA is the cause of amnesic shellfish poisoning in humans caused by consumption of contaminated shellfish (Work et al., 1993; Backer and McGillicuddy, 2006; Kvitek et al., 2008).

HABs have become more frequent and toxic over the last few decades (Glibert et al., 2005; Lefebvre and Robertson, 2010; Sellner et al., 2003). Factors responsible for the increased occurrence could be a combination of natural changes (e.g. species dispersal), anthropogenic changes (e.g. nutrient loading) and/or an improved ability to detect HABs (Glibert et al., 2005). Advances in technology and more frequent sampling contribute to the increased observations of toxic blooms, but cannot account for the total escalation of these events (Glibert et al., 2005). We now know that, due in part to anthropogenic activities, *Pseudo-nitzschia* HABs are becoming increasingly common in areas where they once were rare (Parsons et al., 2002).

The Global Ecology and Oceanography of Harmful Algal Blooms (GEOHAB) program was established to develop a comprehensive understanding of the "mechanisms underlying the population dynamics of harmful algal blooms" (GEOHAB 2008). 'Stratified Systems' is a core research project within GEOHAB that pursues the objective of observing HAB dynamics in highly stratified coastal marine environments. Examples of stratified systems where blooms of *Pseudo-nitzschia* have been observed are in the vicinity of the San Juan Islands (Rines et al., 2002; McManus et al., 2003), Monterey Bay (Ryan et al., 2005; McManus et al., 2008) and Ría de Pontevedra, Spain (Velo-Suárez et al., 2008). Our study site, the northeastern bight of Monterey Bay, is a highly stratified

environment that fits the GEOHAB criteria for the Stratified Systems Core Research Program.

Monterey Bay, California is a monitoring site for HABs where many studies have observed recurring blooms of toxic *Pseudo-nitzschia* (e.g., Fritz et al. 1992; Lefebvre et al., 2002; Bargu et al., 2008; McManus et al., 2008). Diatom species dominate during the upwelling season (Pilskaln et al., 1996; Brzezinski et al., 1997; White and Dugdale, 1997), whereas picoplankton dominate during relaxation (Pilskaln et al., 1996). Domoic acid (DA) is of particular concern in Monterey Bay during the upwelling season, because owing to the high productivity in this area, food chains are short, allowing DA to be rapidly transferred to higher trophic levels (Kvitek et al., 2008). Toxic *Pseudo-nitzschia* are directly consumed by species such as anchovies and mussels. DA is eventually transferred to higher trophic level species such as seabirds, sea lions and humans (Kvitek et al., 2008). HABs in Monterey Bay have resulted in shellfish fishery closures, and marine mammal (Lefebvre et al., 1999) and seabird deaths (Work et al., 1993). The first documented case of domoic acid poisoning among humans occurred in 1987, when afflicted people displayed gastrointestinal and neurological symptoms, some resulting in death (Lefebvre et al., 2002; Backer and McGillicuddy, 2006).

Despite monitoring efforts, HABs are difficult to forecast and there is seldom warning of DA poisoning prior to the onset of obvious symptoms displayed by animals. When there is a toxic phytoplankton bloom with no prior detection, the event is called a “cryptic bloom” (Scholin, personal communication; McManus et al., 2008). The occurrence of cryptic blooms shows the importance of developing methods for determining where there are favorable HAB conditions. In order to accurately predict the toxicity of HABs, it is critical to understand what mechanisms cause blooms to become toxic. Prediction is complicated because *Pseudo-nitzschia* blooms, composed of a species known to be toxic, do not always result in domoic acid poisoning (Dortch et al., 1997).

Studies suggest that nutrients play a role in HAB dynamics. For instance, *Pseudo-nitzschia* will slow their growth rate under conditions of nutrient depletion (Pan et al.,

1996a). Conversely, the addition of nutrients can fuel *Pseudo-nitzschia* blooms (Smith et al., 1990; Trainer et al., 2000; Parsons et al., 2002). However, the relationship between nutrients and HAB dynamics is more complex than simply triggering or terminating blooms. For example, HAB dynamics can also be influenced by factors such as nutrient ratios (Parsons et al., 2002) and nutrient speciation (Hillebrand and Sommer, 1996). Since the stimulation of HABs can be caused by elevated nutrient load, increased occurrence of HABs could be explained by anthropogenic perturbation in the form of excess nutrient loading, and HABs may thus be a signal of our changing environment.

In this contribution we describe the physical and nutrient environment influencing a subsurface layer of *Pseudo-nitzschia* in northeastern Monterey Bay during June 2010 in order to better understand the interrelationships between nutrients and HAB dynamics. Profilers and towed instruments were deployed and laboratory analyses of discrete water samples were conducted to describe the physical and biogeochemical conditions of the sampling site, and to characterize the bloom. Discrete water samples were taken above, within and below the layer.

2. MATERIALS AND METHODS

2.1 STUDY AREA

Monterey Bay is located on the central coast of California (Fig. 1). A non-estuarine embayment (Pennington and Chavez, 2000), Monterey Bay is the largest open bay on the west coast of the United States. The study area is in the northeastern part of Monterey Bay where the upwelling shadow occurs (Graham and Largier, 1997).

The upwelling season along the central California coast extends from March to October (Pennington and Chavez, 2000). During this period, winds are predominantly northwesterly, causing offshore Ekman transport of surface waters along the outer coast. When these surface waters are advected offshore, they are replaced by cold nutrient-rich waters upwelled from as deep as 300 m (Graham and Largier, 1997). A major upwelling center, Point Año Nuevo, is located ~ 30 km north of Monterey Bay (Rosenfeld et al., 1994; Fig. 1). Under upwelling conditions, circulation dynamics cause water in the northern part of the Bay to become separated from the inner-bay, creating an upwelling shadow (Graham, 1993; Graham and Largier, 1997). The water in the upwelling shadow is characterized by long residence times, and is sheltered from wind-induced mixing by local topography, leading to pronounced stratification (Graham, 1993). At periods of 15 to 40 days, the winds can lessen (< 3 m s^{-1}) or reverse direction (Rosenfeld et al., 1994); these periods are termed ‘relaxation’ periods (Fitzwater et al., 2003). During relaxation, upwelling weakens and warm, nutrient-poor California Current water from offshore moves coastward into the Bay (Rosenfeld et al., 1994; Ryan et al., 2009).

The 24-hour time period examined in this study spans from 1400 hours on 27 June to 1400 hours on 28 June 2010 (PDT). During this time we utilized an autonomous profiler, a high-resolution shipboard profiling package, two towed vehicles (Acrobat and ISIIS), multi-frequency acoustics and collected discrete bottle samples.

2.2 ENVIRONMENTAL DATA

Winds are important in determining upwelling potential. Wind velocities (averaged over an eight-minute period and reported hourly) were obtained from the National Data Buoy Center's buoy number 46042, located at 36.789˚N 122.404˚W. Buoy 46042 is located ~45.5 km SW from the profiling sites (Fig. 1).

Tides influence the general oceanographic conditions during the study period. Tidal height was calculated using the pressure sensor on a Sea Bird Electronics model 37SMP CTD positioned 16 m above the bottom proximal to the SeaHorse (see section 2.3.1).

2.3 WATER COLUMN PROFILING

2.3.1 SEAHORSE PROFILER

A Brooke Ocean Technology autonomous SeaHorse profiler, moored at 36.9325˚N, 121.9244˚W, was used to measure water column characteristics (Fig. 1). The water column was profiled between 1 and 15 m depth every 30 minutes. The SeaHorse is slightly positively buoyant, taking measurements from depth to near surface with an average ascent rate of 33 cm s^{-1}, and uses wave energy to ratchet down the mooring line after each profile. The SeaHorse was equipped with a SBE-19*plus* CTD (temperature, salinity, density, and pressure) and a WET Labs WETStar fluorometer (chlorophyll-*a* fluorescence) with a sampling frequency of 4 Hz (average vertical resolution of 8.3 cm). The SeaHorse was located ~7 m from the CTD described in section 2.2.

2.3.2 HIGH-RESOLUTION PROFILER

Additional higher-resolution water column sampling was conducted immediately adjacent to the SeaHorse moored profiler. From 12:15 hours to 15:47 hours on 27 June, a 10 m vessel, the R/V Paragon, was anchored at 36.9324˚N, 121.9246˚W (Fig. 1), and a custom-built profiling package was used to collect high-resolution measurements of the water column from ~ 1 m to ~ 21 m depth every 24 minutes. The high-resolution profiler was designed to be slightly negatively buoyant, resulting in a slow sinking motion disconnected from boat movement. The profiler had an average decent rate of 13.2 cm s^{-1}

and was equipped with a SBE-25 CTD (temperature, salinity, density, and pressure) with a sampling rate of 8 Hz, and a WET Labs ac-9 spectral absorption and attenuation meter (6 Hz) achieving a vertical resolution of 2.2 cm. Following Mobley et al. (2002), we used the absorption at 676 and 650 nm (*ap*676 and *ap*650, respectively) measured by the ac-9 to estimate chlorophyll-*a* concentration (mg m^{-3}):

$$chla = \frac{ap676 - ap650}{0.014} \quad (1)$$

2.4 TOWED VEHICLES

2.4.1 ECHOSOUNDER (SIMRAD 200) AND ISIIS

The water column was also sampled using a combination of acoustics and digital imagery in the vicinity of the moored instruments in order to obtain *in situ* information on planktonic organisms. To collect acoustic backscatter data, an echosounder (Simrad EK-60 at 200 kHz) was side-mounted 1 m below the surface on a second 18 m vessel, the RV Shana Rae, which simultaneously towed the *In Situ* Ichthyoplankton Imaging System (ISIIS) (described in the following paragraph). Acoustic backscatter can be used to estimate distribution and abundance of plankton biomass (Warren et al., 2003). The echosounder recorded continuously while the ship was underway.

ISIIS is an optical, digital imaging system that samples large volumes of water with high resolution (Cowen and Guigand, 2008). ISIIS was towed in an undulating (surface to bottom) fashion, 2.73 to 0.14 km from the profiling sites from 1236 to 1259 hours on 28 June 2010 (Fig. 1). This study was part of a larger project funded by the National Science Foundation (NSF) aimed at understanding lateral mixing dynamics on the shelf of an open coastal system. The transect line described in this paper was selected because it passed closest to the moored profiling sites. The ISIIS captured images of the organisms present in the water column, including those producing the backscatter measured by the echosounders, at a rate of 17 frames per second when towed through the water at 5 knots (2.5 m s^{-1}). ISIIS uses a Piranha II line scan camera from Dalsa, with 50 μm pixel resolution to capture a continuous image. VisionNow software (from Boulder Imaging,

Inc.) breaks up the images collected by ISIIS into 13 cm x 13 cm frames with a 40 cm depth of field. Imaged flocs were identified and measured visually.

2.4.2 ACROBAT

In the vicinity of our profiling site, a SeaScience LTV-50X Acrobat was towed behind a third ~ 9 m vessel, the RV Sheila B, which traveled between 0.4 and 1.2 kts (Fig. 1). The Acrobat profiled in an undulating (near surface to near bottom) fashion to a maximum depth of approximately 25 m. The Acrobat collected temperature, salinity, chlorophyll-*a* and optical backscatter data at 660 nm.

2.5 THIN LAYER CRITERIA

Our thin layer criteria followed those proposed by Dekshenieks et al. (2001). In order to be considered a thin layer, the vertical extent (thickness) of the chlorophyll-*a* peak must be $\leq$ 5 m. The 5 m threshold was chosen because this thickness is the finest-scale vertical resolution achieved by conventional sampling methods (e.g. bottles and nets). The thickness was defined as the depth where the optical signal was half of the peak intensity. Next, the feature must be present in at least 2 consecutive profiles. Third, the intensity of the chlorophyll-*a* peak must be at least 3x the background. The background was determined above and below the feature, where the chlorophyll-*a* concentration is relatively low and invariant.

2.6 DISCRETE WATER SAMPLES

Water samples were collected with a 5-L Aquatic Research Instruments discrete point water-sampling bottle, attached less than 0.2 m from the intake tubes on the shipboard profiler. Decisions to trigger the bottle were made using the real-time depth and fluorescence readings from the profiler. Bottle samples were taken above, within, and below thin layers of fluorescence. Water samples were taken at 1500, 1529, 1547 hours at depths of 9.8, 18.0 and 3.0 m, respectively. Each 5-L water sample was transferred to a carboy and gently mixed to ensure the water was homogeneous before splitting into subsamples for phytoplankton identification and enumeration, as well as analysis of

nutrients, alkaline phosphatase activity, domoic acid and total suspended solids analysis (described in sections 2.6.1 – 2.6.5).

2.6.1 PHYTOPLANKTON IDENTIFICATION AND ENUMERATION

Phytoplankton samples were stored unfixed on ice and processed within 5 hours after returning from the field. Using a Zeiss A1 Axioscope microscope with 40x magnification, phytoplankton were enumerated and identified to genus level in a PhycoTech 0.066-mL phytoplankton counting cell. Triplicate counts were performed for each sample and averaged.

2.6.2 NUTRIENT ANALYSES

Nutrient samples were filtered (acid clean 47-mm diameter, 0.2-µm GH Polypro) within 5 hours after returning from the field. Filtrates were frozen and shipped in acid cleaned bottles to the University of Washington Water Center (Marine Chemistry Laboratory) for analysis. Dissolved inorganic nutrient concentrations (PO_4^{3-}, $Si(OH)_4$, NO_3^-, NO_2^-, NH_4^+), total dissolved nitrogen (TDN) and total dissolved phosphorus (TDP) were analyzed using a Technicon Model AutoAnalyzer II using standard protocols (Valderrama, 1981; UNESCO, 1994). The detection limits of PO_4^{3-}, $Si(OH)_4$, NO_3^-, NO_2^-, NH_4^+, TDN and TDP were 0.02, 0.21, 0.15, 0.01, 0.05, 0.34, and 0.03 µM, respectively, as reported by the Water Center (Krogslund, personal communication).

2.6.3 ALKALINE PHOSPHATASE ACTIVITY

Samples assayed for alkaline phosphatase activity (APA) were filtered through acid-cleaned 47-mm diameter, 0.2-µm GHP filters (volumes ranging from 750-mL to 1 L). Filtered particulates were stored frozen in Petri dishes until analyzed. A filter pore size of 0.2-µm was chosen to examine cell-associated activity for the whole community. APA was analyzed using fluorometric methods similar to Dyhrman and Ruttenberg (2006). APA hydrolyzes the substrate DiFMUP (6,8-difluoro-4-methylumbelliferyl phosphate, Invitrogen®) to produce a fluorescent product, DiFMU (6,8-difluoro-7-hydroxy-4-methylcoumarin). The fluorescence (excitation at 360 nm and 460 nm emission) was measured on a BioTek Synergy HT Plate Reader at a temperature of 25˚C. APA was

determined using the linear response range of standards made using a dilution series of the fluorescent compound DiFMU. Blanks were prepared prior to assays and stored frozen in Petri dishes until analyzed alongside samples.

2.6.4 DOMOIC ACID

Particulate domoic acid samples (each 750-mL) were filtered onto 47-mm diameter, 0.2-µm GHP filters. Dissolved domoic acid samples were filtered through a 47-mm GF/F filter and frozen in acid washed bottles. Samples were analyzed using the method described by Wang et al. (2007), modified for Selected Ion Monitoring on an Agilent 6130 LC/MS.

2.6.5 TOTAL SUSPENDED SOLIDS

Total suspended solid samples (each 750-mL) were filtered through pre-weighed 47-mm diameter, 0.2-µm GHP filters. The filters were dried until the daily measured post-weighs were reproducible within less than 0.16%. Total suspended solids (TSS) concentrations were calculated by taking the difference between the pre-weight and the post-weight divided by the volume of water filtered.

3. RESULTS

3.1 ENVIRONMENTAL MEASUREMENTS

From 1400 hours on 27 June to 0100 hours on 28 June winds were from the northwest with an average velocity of 4.6 m s^{-1} (Fig. 2a). During this time winds weakened from a maximum of 6.6 m s^{-1} to 1.1 m s^{-1}. After 0100 hours on 28 June, the winds were variable and not as strong (average velocity of 1.5 ms^{-1}). Winds had been consistently from the northwest starting from 13 June 2010.

Monterey Bay experiences mixed, semi-diurnal tides. The tidal range during the study period was 2.4 m (Fig. 2b). High tide was at 2323 hours on 27 June and low tide was at 0632 hours on 28 June. The full moon occurred on 26 June, thus the sampling occurred during spring tide conditions.

3.2 PROFILER OBSERVATIONS

The water column was stratified as evidenced by the relatively invariant isopycnals across time until ~0800 hours on 28 June (Fig. 2c). The mixing that occurred after 0800 hours because the change in water circulation lags behind the change in winds from upwelling favorable to relaxation. From 2000 hours on 27 June to 0300 hours on 28 June, either diurnal surface cooling or advection caused the isotherms to shoal (Fig. 2d). An intense, subsurface *Pseudo-nitzschia* layer was present throughout the entire study period (Fig. 2d). From 1400 to 2200 hours, the layer had an average thickness of 6.36 m and depth of 8.47 m. From 2200 to 0800 hours, the layer thinned (average = 3.6 m) and shoaled slightly to a mean depth of 7.2 m. After 0800 hours the layer broadened (to depths beyond those measured by the SeaHorse) and deepened (mean depth of 10.5 m).

High-resolution profiler measurements were examined for a 2-hr period, from 1400 to 1600 hours on 27 June (Fig. 2e-i). The water column was stratified and a thin *Pseudo-nitzschia* layer persisted during these two hours, with an average depth of 8.1 m and thickness of 2.69 m. Three bottle samples, collected ~24 minutes apart during this time

period, were taken above, within, and below the layer (Table 1). Results from theses samples are described in sections 3.4 – 3.5.

3.3 ACOUSTICS AND ISIIS

The 200-kHz echosounder data shows high acoustic backscatter roughly 8 m below the surface (Fig. 3). The dark red signal that shoals with distance across-shelf is the trace of the seafloor. The high backscatter layer broadens and deepens toward the shallow (inshore) end of the transect. The depth at which the high backscatter occurs corresponds with that of the *Pseudo-nitzschia* layer detected by the SeaHorse and shipboard profiler, as well as by data obtained from the bottle samples.

Along this same across-shelf transect, ISIIS images were captured at all depths. To identify specific constituents of the water column above, within, and below the thin *Pseudo-nitzschia* layer, one image is shown from each of these regions within the water column (Fig. 4). Above the layer, small flocs were abundant in the image, each with a maximum surface area of about 1 cm^2 (Fig. 4a), and many individual cells. Within the thin layer itself there were fewer, but larger flocs (maximum of ~ 2 cm diameter and a surface area of 2 cm^2; Fig. 4b). Below the layer, there were two large flocs (1.5 cm^2), four small flocs (0.5 cm^2) and many small, individual cells similar to those observed in the image from above the layer (Fig. 4c).

3.4 CHEMISTRY OF THE THIN LAYER

Discrete water samples were taken above, within and below the thin layer (Figure 5). Total dissolved nitrogen (TDN) and total dissolved phosphorus (TDP) are the sum of both the dissolved inorganic and organic forms of nitrogen and phosphorus, respectively. The TDN : TDP ratio was 167% and 272% higher within the layer compared to above and below, respectively (Table 1; Fig. 5a). TDN : TDP ratios from above and within the layer were higher than the Redfield ratio, while TDN : TDP ratios from below the layer were lower than the Redfield ratio.

TDP and DIP concentrations displayed typical nutrient profile shapes, in which concentrations increase with depth (Fig. 5b). The inorganic portion of TDP pool increases with depth, and DIP concentrations constitute 39, 50 and 88% of TDP in samples from above, within and below the layer, respectively. Silicic acid ($Si(OH)_4$) also has a typical nutrient profile shape, in which concentrations increase with depth (Table 1). Alkaline phosphatase activity (APA) decreases with depth (Fig. 5c).

Concentrations of dissolved organic nitrogen (DON) were elevated within the layer (Fig. 5d), with concentrations exceeding DIN by 257% and 279% above and below the layer, respectively. Similarly, total suspended solids (TSS) concentrations within the layer were higher than TSS in waters above and below the layer.

Ratios of dissolved inorganic nitrogen (DIN: NO_3^-+NO_2^-+NH_4^+) to dissolved inorganic phosphorus (DIP: PO_4^{3-}) concentrations were higher within the layer compared to DIN : DIP ratios above or below the layer (Table 1; Fig. 5e). DIN : DIP ratios at all three depths were below the Redfield ratio of 16 N : 1 P.

3.5 *PSEUDO-NITZSCHIA* AND DOMOIC ACID

Phytoplankton counts showed that the water column between 3 and 18 m was dominated by *Pseudo-nitzschia* during the sampling period. Concentrations ranged from 1172±107 to 7783±948 cell mL^{-1}, levels which exceed the threshold defined for a harmful algal bloom (Lefebvre et al., 2002). Other genera, such as *Chaetoceros spp.*, were present as well, but collectively were < 152 cells mL^{-1}, an order of magnitude lower than *Pseudo-nitzschia* concentrations (data not shown). Compared to waters above or below the thin layer, concentrations of *Pseudo-nitzschia* within the layer were 682% and 500% higher, respectively (Table 1; Fig. 5f). All depths had moderate concentrations of particulate domoic acid (Table 1; Fig. 5g). The concentration of particulate domoic acid concentrations within the layer was 237% and 162% higher than those above or below the layer, respectively. The dissolved domoic acid was also highest within the layer when compared to water above and below the layer (Table 1; Fig. 5h). This concentration of

Pseudo-nitzschia, along with the presence of domoic acid in the thin layer, suggests that this feature can be considered a HAB.

A nearly linear relationship exists between the concentration of *Pseudo-nitzschia* cells determined from all phytoplankton counts of discrete bottle samples and the chlorophyll-*a* concentration calculated from the profiler ac-9 signal (equation (1); Fig. 6), indicating that the chlorophyll-*a* signal measured by the profiler is dominated by *Pseudo-nitzschia*. Although this paper only focused on a 24 hour time period, our cruise was thirteen days long. Fourteen additional samples associated with layers were taken during this time and all data were used to investigate this relationship. Based on both the *Pseudo-nitzschia* counts and the strong relationship between *Pseudo-nitzschia* and ac-9 absorption, we conclude that the layer defined by the chlorophyll-*a* fluorescence signal is composed of *Pseudo-nitzschia.*

4. DISCUSSION

4.1 ACOUSTIC DETECTION OF FLOCS OF *PSEUDO-NITZSCHIA*

A 200-kHz acoustic signal is expected to scatter off of objects in the size range of small zooplankton, including invertebrate larvae (~300 μm and larger; Clay and Medwin, 1977). Therefore, individual *Pseudo-nitzschia* cells (approximate size 100 μm) could not be detected with the 200-kHz echosounder such as the one used in this study. However, the observed flocs detected by the towed ISIIS in the layer dominated by *Pseudo-nitzschia* cells occurred at the pycnocline as aggregates with diameters on the order of 1-2 cm. With these larger scattering targets, it is possible that the acoustic backscatter signal observed at the pycnocline was caused by flocs of *Pseudo-nitzschia*, in concentrations of 0.142 flocs cm^{-2} (D. McGehee, pers. comm.). Another possibility is that the high acoustic scattering signal within the *Pseudo-nitzschia* layer resulted from oxygen bubbles in the flocs, or larger organisms attracted to the layer (J. Warren, pers. comm.), though few of the latter were observed in any of the imagery. Some of the ISIIS images show appendicularians in the flocs. However, appendicularians were most abundant below the high backscatter layer. Zooplankton, principally copepods, were observed throughout the water column, and were most abundant above the high acoustic backscatter layer (0-5 m depth).

Images from the towed ISIIS show that particulates in the subsurface layer are dominantly composed of flocs. Phytoplankton counts from bottle samples reveal that *Pseudo-nitzschia* dominate the water column, and are most abundant within the subsurface layer. It should be noted that sampling with the Aquatic Research Instruments bottle used in this study would likely disrupt the fragile flocs. In the absence of direct physical sampling of flocs, we argue on the basis of the images of the ISIIS, fluorescence data from profilers, and phytoplankton counts from discrete water samples, that these flocs are primarily composed of *Pseudo-nitzschia.* Evidence for *Pseudo-nitzschia* flocs can be seen in sediment trap data from this region (Vigilant and Silver, 2007; Olivieri, 1996; Dortch et al., 1997; Parsons et al., 2002) and by the observations of Sekula-Wood et al. (2011) in the nearby Santa Barbara Channel, suggesting that this is a prevalent

phenomenon in this region. Alldredge and Gotschalk (1990) described a diatom floc (mostly diatoms by volume and > 30% diatoms and frustules by count) from Southern California as being large (2-3 cm in length), 'comet-shaped', and porous. This description is consistent with the ISIIS image observations in this study.

For diatom flocs to occur, cells must come into physical contact with one another (collisions) and adhere (Alldredge and Gotschalk, 1989). One way diatoms adhere to one another is through transparent exopolymer particles (TEP; Sarthou et al., 2005) such as mucus (Alldredge and Gotschalk, 1989). Alldredge and Gotschalk (1989) observed that higher concentrations of extracellular mucus were present when *Pseudo-nitzschia* cells were present as flocs, and speculated that the increased stickiness promoted by higher TEP concentration caused increased flocculation. It is known that under physiological stress, TEP production increases (Drapeau et al., 1994). Thus, under conditions that create physiological stress, increased TEP production by diatoms may result in increased flocculation. One common stressor for *Pseudo-nitzschia* cells is nutrient limitation (Smetacek, 1985; Alldredge and Gotschalk, 1989; Drapeau et al., 1994), and our data set allowed us to specifically examine the nutrient regime within the layer where the *Pseudo-nitzschia* flocs occurred to evaluate whether nutrient levels may have triggered floc formation.

There are nutritional benefits to *Pseudo-nitzschia* when cells flocculate. Flocs could increase nutrient uptake by altering fluid flow. For example, Logan and Alldredge (1989) calculated that aggregated (flocculated) cells could absorb nutrients up to 2.1x faster than individual cells. In addition to fluid flow, microbes within the flocs release bioavailable nutrients (Alldredge and Silver, 1988). Studies have shown that the interstitial nutrient concentration in flocs can be higher than in the surrounding water (Alldredge and Silver, 1988). For the subsurface diatom layer observed in this study, we hypothesize that the presence of flocs indicates that the cells in the layer may have been experiencing nutrient stress.

Diatom flocculation most commonly occurs at the termination of a bloom (Gotschalk and Alldredge, 1989), or when there is little or no growth (Calleja, 1984; Alldredge and Silver, 1988). Flocs have been observed to settle out of the water column and potentially transport toxins to the benthic community (Kvitek et al., 2008). Not all flocs will sink immediately; they can persist in the water column for days (Sarthou et al., 2005). For this study, *Pseudo-nitzschia* flocs above the layer displayed evidence of sinking (tails on the flocs), whereas tails are not present on flocs within or below the layer. It is possible that flocs above the *Pseudo-nitzschia* layer reached a density surface (in the pycnocline) that slowed their sinking rate, allowing the flocs to form a layer. Alldredge and Crocker (1995) hypothesize that diatom flocs can achieve neutral buoyancy when lower density mucus replaces seawater within the floc, thus stopping sinking. In their study, the aggregates were primarily found in the pycnocline.

There are many similarities between the thin layer described in this study and a thin layer observed by Alldredge et al. (2002) in the San Juan Islands, Washington. In the latter study, the thin layer was primarily composed of flocs of *Odontella longicruris* (chain forming diatom) that were > 1 cm in diameter, had an average thickness of 60 cm, and lasted more than 24 hours at a depth of 5 to 7 m. The pycnocline (3 to 5 m) had a strength of $\Delta 1\sigma_t$. The thin layer we focus on in this paper was much thicker, but was also associated with a density surface. Alldredge et al. (2002) observed a diatom bloom within and above the layer and showed differential aggregation. The current study shows *Pseudo-nitzschia* dominated the water column. The tails on the flocs above the layer indicate that the bloom could have been in the surface waters prior to our observations. Alldredge et al. (2002) may thus have observed a similar situation to that observed in our study, yet at an earlier stage of bloom succession.

Diatom flocs that accumulate on density surfaces might occur frequently. Pilskaln et al. (1998) found aggregates on the outer edge of Monterey Bay that were associated with density discontinuity layers. Similarly, in the Adriatic Sea, mucilage (suspended gelatinous material where flocs are one form) has caused problems for the economy (tourism and fisheries). In fact, occurrences of mucilage were observed as early as 1729

(Innamorati, 1995), and are thought to start as marine snow and progress to large clouds (Fogg, 1995). The marine snow is composed of diatom flocs and has been associated with the pycnocline, where the flocs accumulate (Mingazzini and Thake, 1995). Specifically, *Nitzschia* and *Skeletonema spp*. are "usually associated with the Adriatic mucilage" (Fogg, 1995). The diatom *Chaetoceros* has also been found within the mucilage aggregates, but are not dominant (Innamorati, 1995). Myklestad (1995) points to nutrient stress as a possible cause of polysaccharide release by *Chaetoceros*; polysaccharides are the precursors of TEP (Passow and Alldredge, 1994). Aggregations have also been observed in the Tyrrhenian Sea, Toscana coast, and Sicilian coast (Minagazzini and Thake, 1995).

4.2 DOMOIC ACID

High levels of dissolved domoic acid (DA) were observed within the layer (Fig. 5c; Table 1) indicating that the cells associated with the bloom and flocs observed were actively leaking DA. The highest dissolved DA level observed (123.33 nM) is substantially higher than the few reported values from field samples (c.f. Bargu et al. 2006; Caron et al. 2010), but is comparable to the reported value of ~40 ug L^{-1} (128 nM) for Monterey Bay in 2000 (Doucette et al. 2002). Despite the relatively high levels, there is no clear evidence that dissolved DA at these concentrations directly impacts other organisms. For example, Bargu et al. (2006) demonstrated feeding deterrence in krill (*Euphasia pacifica*) at ~1,282 nM, whereas Olson and Lessard (2010) showed no direct inhibition of microzooplankton or dinoflagellates at DA concentrations of 50 and 80 nM.

A study in San Diego, California (Scripps Pier) reported *Pseudo-nitzschia* concentrations of 7.7 x 10^4 cells L^{-1} with pDA concentrations of 1.98 μg L^{-1} in February 2004, which resulted in sea lion strandings (Busse et al., 2006). Schnetzer et al. (2007) reported the highest concentrations of pDA yet observed on the west coast, 12.7 μg L^{-1} with up to 5.3 x 10^4 cells L^{-1} during 2003-2004, and linked the elevated surface concentrations of pDA to subsequent elevated concentrations in sediment traps. Schnetzer et al. (2007) also reported an inverse correlation between toxin levels and macronutrients, suggesting nutrient stress as an environmental factor leading to toxic blooms. Previous laboratory

experiments have shown that the production rate of DA by *Pseudo-nitzschia* can be controlled by the availability of macronutrients (Pan et al., 1996a,b,c) and micronutrients (Maldonado et al., 2002), and suggest nutrient stress as a possible cause of increased toxicity (Bates et al., 1991; Fehling et al., 2004). Increased DA production by *Pseudo-nitzschia* cells was observed to occur under conditions of phosphate (Pan et al., 1996a) and silicate limitation (Bates et al., 1991; Pan et al., 1996b,c). Because DA is an amino acid, and thus contains nitrogen, it has been argued that under conditions of nitrogen limitation DA would not be produced (Bates et al., 1991). Kudela et al. (2004) found low levels of DA in nitrogen-limited cultures, consistent with this argument. In fact, DA concentrations in nitrogen-limited cultures were orders of magnitude lower than those observed in Si-limited cultures (Kudela et al., 2004). Thus, it is likely the *Pseudo-nitzschia* cells in the layer we observed were producing DA in response to nutrient stress, but were limited by a nutrient other than nitrogen. Pan et al., (1996a) observed increased toxicity of *Pseudo-nitzschia* under phosphate limited conditions in culture studies, and we next examine whether the flocculated cells growing in the subsurface layer might have been experiencing phosphate stress.

4.3 NUTRIENTS

Our results suggest that phosphate stress is responsible for the formation of *Pseudo-nitzschia* flocs, and possibly also for the increased bloom toxicity in the subsurface *Pseudo-nitzschia* layer we observed in Monterey Bay. This conclusion is based on the presence of flocs in a layer that also is characterized by TDN : TDP ratios that exceed the Redfield Ratio, the presence of APA, and high domoic acid concentrations. Each of these factors is discussed in more detail in the following paragraphs.

Dissolved organic nitrogen (DON) concentrations were > 2x higher within the layer than above or below (Fig. 5h). Bronk et al. (1994) found that DON released by phytoplankton equates to between 25 - 40% of the dissolved inorganic nitrogen (DIN) that was taken up by the cells. Mechanisms of DON release by phytoplankton include passive exudation or release due to grazing (Bronk and Ward, 1999). The accumulation of DON observed within the layer suggests that the high concentrations of *Pseudo-nitzschia* represent *in*

situ growth, as opposed to the cells being advected into the layer from another area. In addition, the fact that winds were consistently from the northwest beginning 14 days prior to the study, causing the upwelling shadow where our study site is located, to be separated from other waters, also makes it unlikely that cells were advected to this location from elsewhere.

Dissolved silicon in the form of silicic acid ($Si(OH)_4$) is required by diatoms to synthesize their tests. It is generally thought that diatoms require an uptake ratio of $Si(OH)_4$: DIN > 1 : 1 (Brzezinski, 1985). However, it is possible that *Pseudo-nitzschia* are able to survive with lower $Si(OH)_4$: DIN ratios (Marchetti et al., 2004) because, compared to other diatoms, *Pseudo-nitzschia* cell structures require less silica (Marchetti et al., 2004). For the layer we sampled, $Si(OH)_4$: DIN ratios exceeded 1 : 1 both at the surface and below the layer, indicating that ample silica was available in the water column. The ratio within the layer was < 1 : 1 (0.85), lower than the threshold ratio for most diatoms, but possibly still within the range favorable for *Pseudo-nitzschia*. Anderson et al. (2006) found the highest abundance of *Pseudo-nitzschia* was associated with the lowest $Si(OH)_4$: NO_3^- and $Si(OH)_4$: PO_4^{3-} ratios. In our study, the *Pseudo-nitzschia* layer had a lower $Si(OH)_4$: NO_3^- ratio than waters above or below the layer, implying that there were low levels of silicic acid relative to nitrate. Pan et al. (1996c) found that the $Si(OH)_4$: NO_3^- ratio is about 0.68 in Si-limited areas, and about 2 in Si-replete areas. The ratio for the thin layer observed in this study falls between these two extremes. On the other hand, $Si(OH)_4$: PO_4^{3-} ratio in the layer was not the lowest (relative to ratios above and below the layer), suggesting that there was more $Si(OH)_4$ relative to PO_4^{3-}.

We consider the possibility that the *Pseudo-nitzschia* in the subsurface layer were phosphate stressed. Traditionally, dissolved inorganic phosphorus (DIP) and dissolved inorganic nitrogen (DIN) are examined to infer nutrient limitation based on the Redfield ratio (Kwon et al., 2011). The DIN : DIP ratios that we observed (Table 1; Fig. 5d) would lead us to conclude that nitrogen is limiting, because the DIN : DIP ratios are lower than the Redfield ratio. However, when we include dissolved organic phosphorus (DOP) and nitrogen (DON), we observed that TDN : TDP ratios (Table 1; Fig. 5e) exceed the

Redfield ratio, which implies that phosphate may be functioning as the limiting nutrient. Many phytoplankton produce enzymes that hydrolytically cleave phosphate from DOP, allowing it to become bioavailable (e.g., Chróst, 1991). One such enzyme is alkaline phosphatase (AP), which is widely used to determine the phosphate-stress status of phytoplankton (e.g., Hoppe, 2003). Alkaline phosphatase activity (APA) increases when DIP concentrations fall below a threshold level (Dyhrman and Palenik 1999; Dyhrman and Ruttenberg 2006; Ou et al., 2006). In this study, we observed that APA decreases with depth, implying that phosphate stress was higher in the upper water column (Fig. 5g). DIP concentrations and APA display an inverse relationship, implying that availability of phosphate affected expression of APA in *Pseudo-nitzschia*. This relationship occurs because when DIP levels are sufficient, organisms are not induced to produce the APA that would enable them to convert DOP to bioavailable DIP, and vise versa. The presence of flocs, APA, TDN:TDP ratios that exceed the Redfield ratio, and high DA concentrations within the *Pseudo-nitzschia* layer suggest that phosphate stress is responsible for the flocs observed in Monterey Bay, and possibly also for the bloom toxicity in the subsurface *Pseudo-nitzschia* layer we observed.

Although phosphate stress appears to be playing an important role in HAB dynamics in Monterey Bay, other nutrients, such as trace metals, can also be important in bloom toxicity (Rue and Bruland, 2001). Thus, we examine an alternate hypothesis, which is that bottom sediments played a role in bloom toxicity. Domoic acid chelates trace metals such as iron and copper (Rue and Bruland, 2001); trace metals typically are present in higher concentrations in seafloor sediment relative to the water column. DA production could be a response to iron limitation. DA binds to iron, solubilizing the iron and allowing it to become bioavailable. On the other hand, cells might also produce DA in response to copper toxicity; DA binds with free copper decreasing copper bioavailability, and thus reducing toxicity (Rue and Bruland, 2001). The fact that the isopycnals deepened and intersected with the seafloor at location #2 along the Acrobat transect (Fig. 7) makes it possible to envisage a potential role for bottom sediments in promoting bloom toxicity. Deepening of the isopycnals towards the inshore end of the transect coincided with increased acoustic backscatter (Fig. 5). Further offshore, both the isopycnals and the

optical backscatter layer were compressed (Fig. 7). However, the chlorophyll-*a* layer observed along this transect stays confined within isopycnals that do no intersect the seafloor. The co-location of the peaks in chlorophyll-a and acoustic backscatter suggests that scattering here is dominated by *Pseudo-nitzschia* flocs. Optical backscatter levels were slightly elevated between the *Pseudo-nitzschia* layer and the seafloor at the location designated by the arrow in Fig. 7, whereas the chlorophyll-*a* remained low. The elevated backscatter in this intervening region suggests that sediment may have been mobilized into the water column.

Johnson et al. (1999) found that sediments can be resuspended during strong upwelling events. We observed the highest concentration of total suspended solids (TSS) within the layer compared to above or below and, given the patterns of the isopycnals described above, it is possible that the higher TSS observed within the layer is caused, at least in part by resuspended sediments. Higher concentrations of cells could also contribute to the increased TSS observed within the layer. The *Pseudo-nitzschia* in the subsurface layer thus may be producing DA in response to this resuspended sediment, either to acquire needed nutrients such as iron, or to protect themselves from toxic metals such as copper. In this case, the DA produced at the inshore site may then have spread throughout the layer (possibly through advection), resulting in the high DA values measured further along the transect at our discrete water sampling site. Alternatively, iron might have been entrained along isopycnals and transported seaward, leading to increased bloom toxicity throughout the study area as cells produce DA to increase Fe bioavailability. Similarly, Ryan et al. (this issue) found surface *Pseudo-nitzschia* were most toxic when in contact with resuspended sediment, and these authors believe that this sediment originated from the shelf bottom boundary layer. Thus, phosphate stress, trace metals or both, could be playing a role in bloom toxicity at the study site. Our data set does not allow us to resolve which effect is dominant in triggering the bloom observed.

A number of studies have documented that the nutrient limitation regime can shift on various time-scales for a variety of reasons, and that drivers of these shifts can be both natural and anthropogenic. For example, Karl (2000) argues that open oceanic areas have

undergone nutrient limitation shifts from nitrogen to phosphorus within the past two decades due to increased nitrogen fixation. In addition to the biological addition of nitrogen through fixation, anthropogenic activities (such as fossil fuel combustion) increase nitrogen emissions to the atmosphere. This nitrogen is subsequently deposited on the sea surface (Krishnamurthy et al., 2007) with little effect on phosphorus (Duce et al., 2008). In the future, if the quantity of nitrogen deposition increases through this or other processes, marine systems could be driven more towards phosphorus limitation (Krishnamurthy et al., 2007), thereby increasing the occurrence of toxic algal blooms.

5. CONCLUSIONS

This study focused on the role that nutrients played in the generation of a toxic *Pseudo-nitzschia* bloom in northeastern Monterey Bay. The bloom was confined to a subsurface layer, contained high levels of domoic acid, and the cells comprising the bloom were mostly aggregated in flocs, the size and abundance of which made the layer detectable by an acoustic echosounder and the ISIIS. The presence of alkaline phosphatase activity (APA) and TDN : TDP ratios in excess of the Redfield ratio suggest that the subsurface *Pseudo-nitzschia* bloom sampled in this study site was most likely phosphate stressed. The *Pseudo-nitzschia* cells may have formed flocs in the surface waters in response to phosphate stress, causing them subsequently to settle to the pycnocline. The DA produced by the cells observed in this study may also have been in response to phosphate stress. Alternatively, trace metals within resuspended sediments might have played a role in causing the bloom toxicity observed in this study. A better understanding of the role of sediment resuspension and phosphate stress in triggering HABs is required in order to more confidently assign causative factors to development of HABs, which would then permit more accurate forecasting of such events. It is also possible that the combined occurrence of phosphate stress and elevated trace metal concentrations from resuspended sediments could enhance the formation of toxic blooms. While other regions could have different conditions that affect HAB dynamics, if phosphate stress is found to be widely important in bloom toxicity, we could anticipate the occurrence of more toxic blooms in the future as anthropogenic nutrient inputs alter nutrient ratios in the direction of higher N : P ratios.

TABLE 1. SUMMARY OF THE THREE DISCRETE SAMPLES FROM ABOVE, WITHIN AND BELOW THE LAYER.

Summary of the three samples from above, within and below the thin layer. Sampling time is in local standard time (PST). Samples were analyzed for particulate domoic acid (pDA), dissolved domoic acid (dDA), total suspended solids (TSS) and silicic acid concentrations. The ratios for dissolved inorganic nitrogen to dissolved inorganic phosphorus (DIN : DIP) and total dissolved nitrogen to total dissolved phosphorus (TDN : TDP) were calculated.

	Time	*Pseudo-nitzschia* (cells mL^{-1})	pDA (ng L^{-1})	dDA (nM)	DIN: DIP	TDN: TDP	TSS (mg L^{-1})	Silicic acid (μM)
Above	15:47	1172	1059	7.82	4.13	25.28	9.98	1.53
Within	15:00	7783	1716	123.33	14.47	42.13	14.30	4.19
Below	15:29	1576	723	22.82	11.90	15.47	11.80	20.38

* *Pseudo-nitzschia* counts are the mean over three samples with a standard deviation of 107, 948 and 675 for above, within and below the layer, respectively. No standard deviation is reported for DA because replicate samples were unavailable. DIN : DIP has an analytical standard deviation of 0.16. Precision of TDN : TDP could not be calculated because analytical uncertainties were not available from the UW Water Center. TSS has a standard deviation of less than 7×10^{-5} between the replicate measurements for the three depths. Silicic acid has standard deviation of 0.19 using analytical uncertainties.

FIGURE 1. MAP OF MONTEREY BAY STUDY SITE

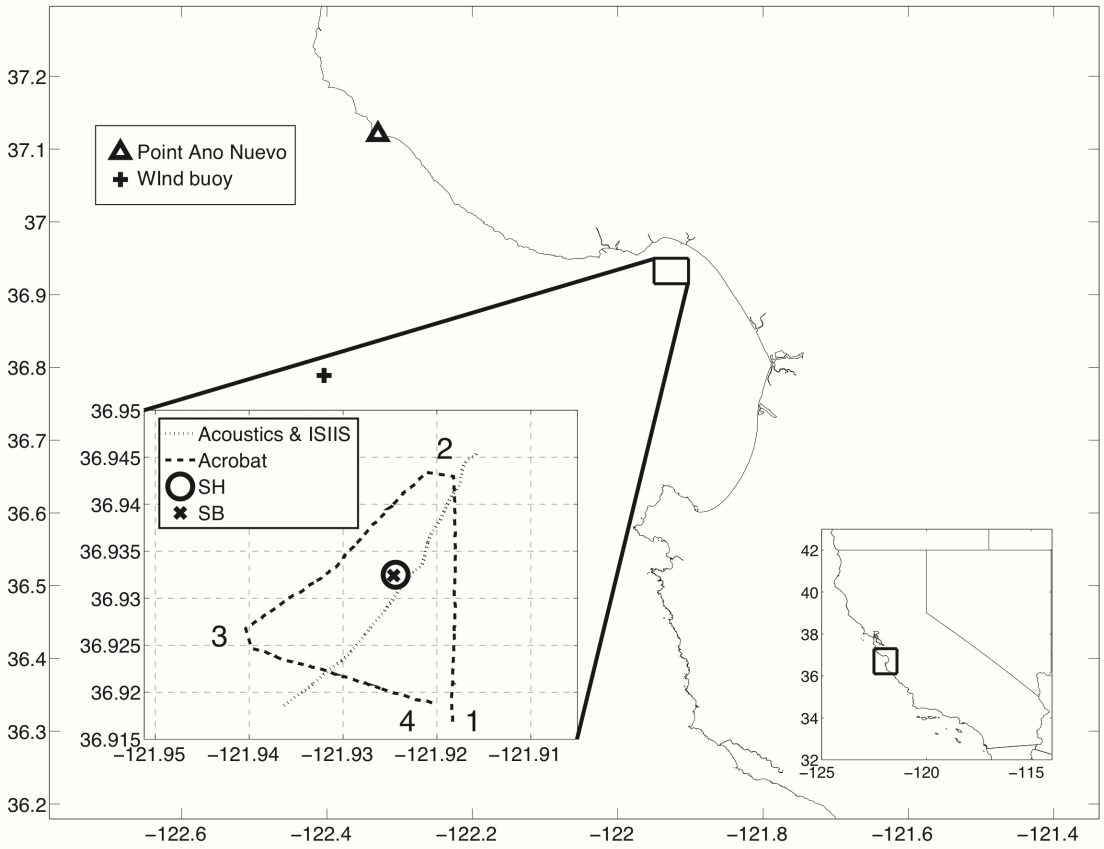

Map of Monterey Bay study site, showing transect paths of the echosounder/ ISIIS and Acrobat, as well as the locations of the SeaHorse (SH) mooring and shipboard (SB) profiling station. The CTD determining tidal height was located ~ 7 m from the SH. Numbers 1-4 indicate positions on the Acrobat transect and are referred to in Figure 8. Triangle is Point Año Nuevo and the plus sign is the location of the wind buoy. Inset map shows the location of Monterey Bay along California coast.

FIGURE 2. SEAHORSE AND SHIPBOARD PROFILERS

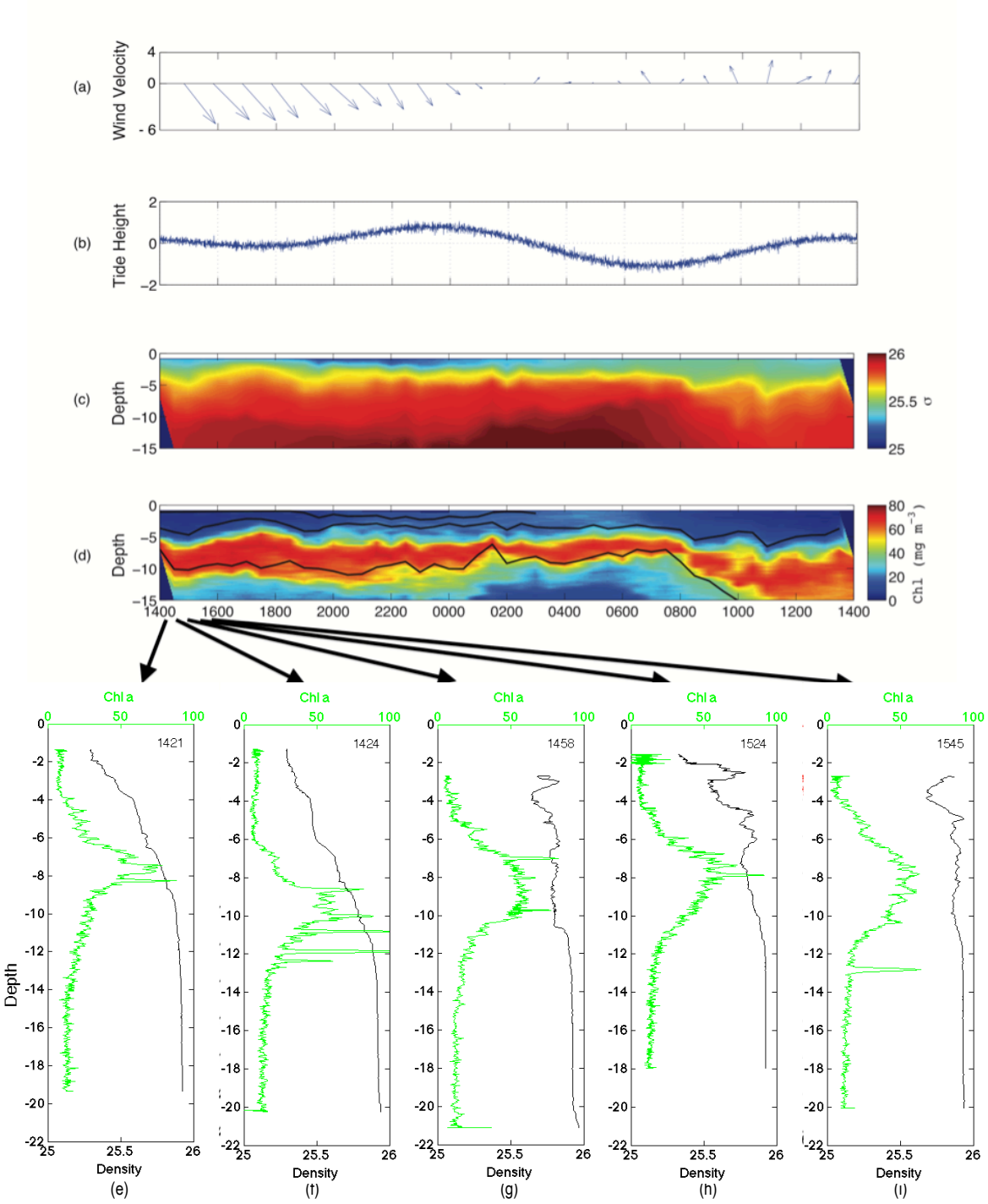

SeaHorse and shipboard profiler data. Time series from 14:00 hours on 27 June to 14:00 hours on 28 June 2010 of: (a) wind velocity (m s^{-1}; arrows point in heading direction), (b) tide height (m), and SeaHorse profiler and mooring measurements of (c) density (kg m^{-3}) and (d) chlorophyll-*a* concentration (mg m^{-3}), with 14, 12.5 and 11˚C isotherms overlaid. Shipboard profiles of chlorophyll-*a* (mg m^{-3}) and density from 27 June at (e) 14:21 hours, (f) 14:24 hours, (g) 14:58 hours, (h) 15:24 hours and (i) 15:45 hours.

FIGURE 3. ACROSS-SHELF TRANSECT OF SIMRAD 200 KHZ ECHOSOUNDER BACKSCATTER

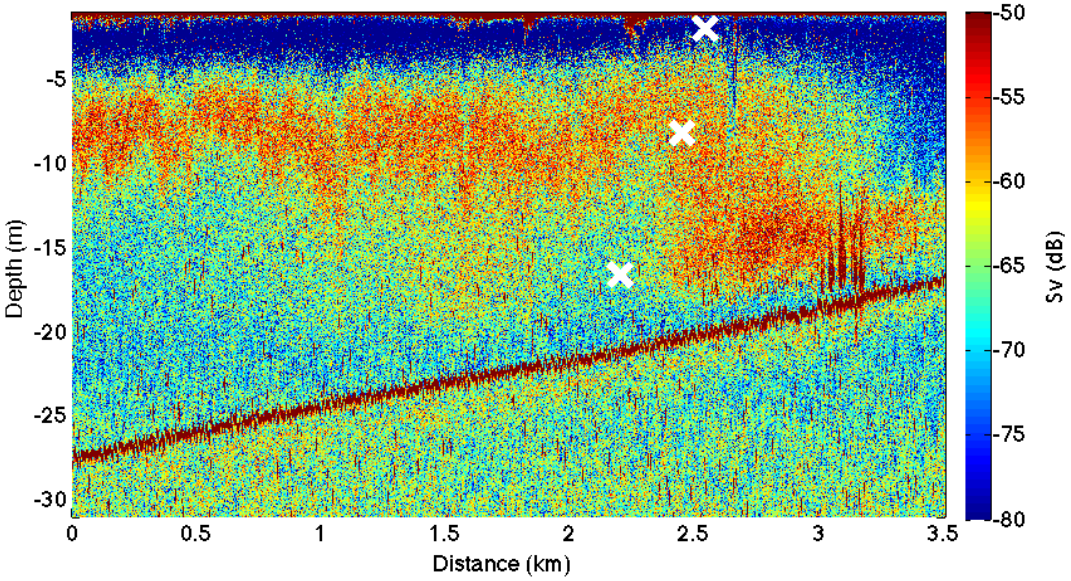

Across-shelf transect of Simrad 200 kHz echosounder backscatter (dB). X's mark where the *In Situ* Ichthyoplankton Imaging System (ISIIS) images were taken. Distance was calculated from the start of the southwest end of the transect (see Fig. 1). The linearly increasing scattering at depth is the trace of the seafloor.

FIGURE 4. ISIIS IMAGES

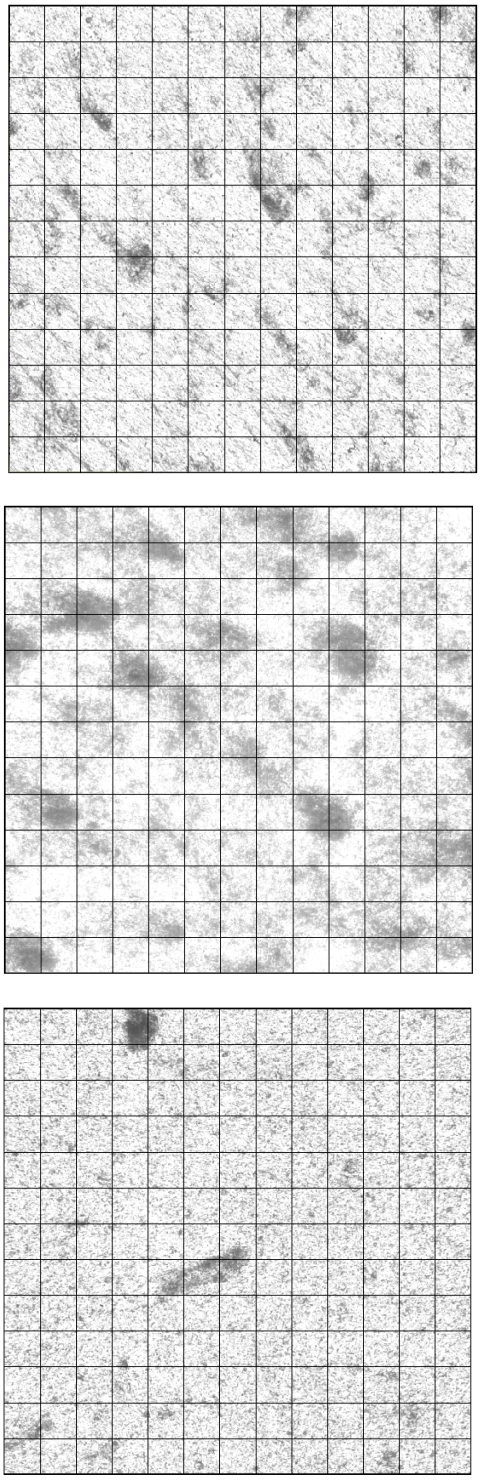

(a)

(b)

(c)

In Situ Ichthyoplankton Imaging System images (ISIIS). *In Situ* Ichthyoplankton Imaging System photos were taken from an across-shelf transect. Photos were captured (a) above, (b) within, and (c) below the layer. Small flocs were abundant above, large flocs were

present within and a mixture of small and large flocs were found below the layer. Tails are visible on the flocs above the layer. Each photo is 13x13 cm with a 30 cm depth of field. Each individual box is 1 cm^2.

FIGURE 5. DEPTH PROFILE OF DISCRETE BOTTLE SAMPLES

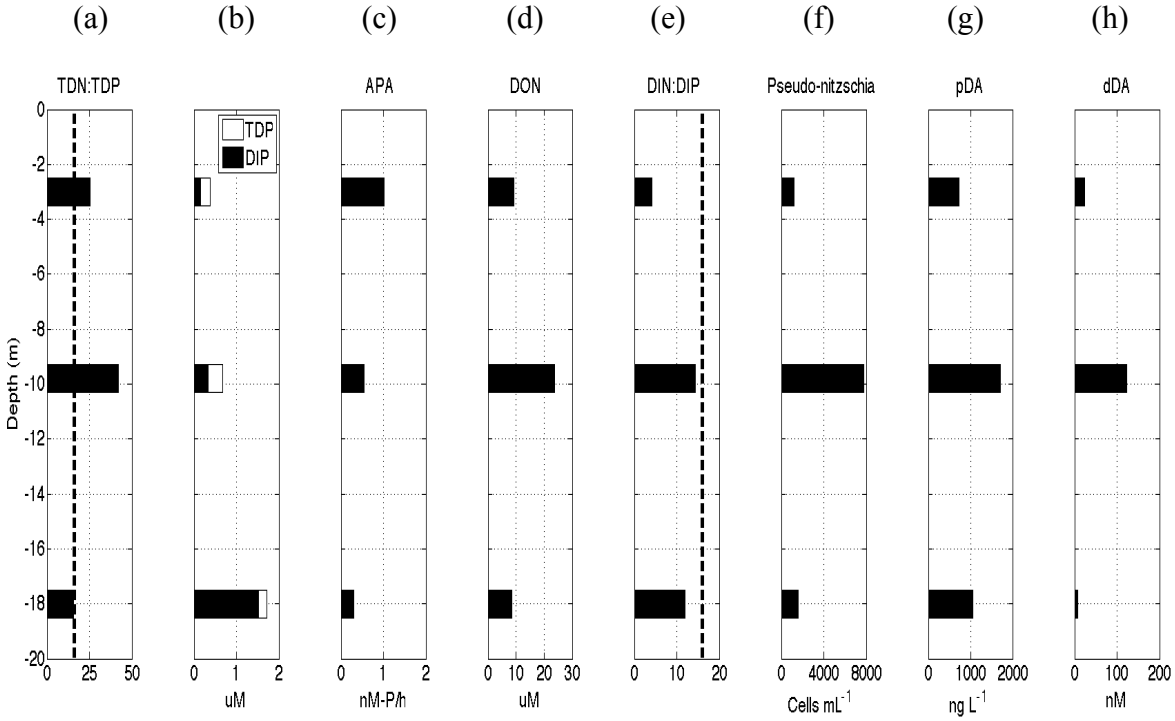

Depth profiles of data from discrete bottle samples taken at 15:00 hours, 15:29 hours and 15:47 hours on 27 June 2010. Depth profile of: (a) *Pseudo-nitzschia* concentrations (cells mL^{-1}), (b) particulate domoic acid (ng L^{-1}), (c) DIN : DIP, (d) TDN : TDP, (e) TDP and DIP (µM), (f) APA (nM-P hr^{-1}) and (g) DON (µM). Red vertical lines indicate the Redfield ratio of 16 : 1.

FIGURE 6. CORRELATION PLOT OF *PSEUDO-NITZSCHIA* CONCENTRATION VERSUS CHLOROPHYLL-*A* CONCENTRATION

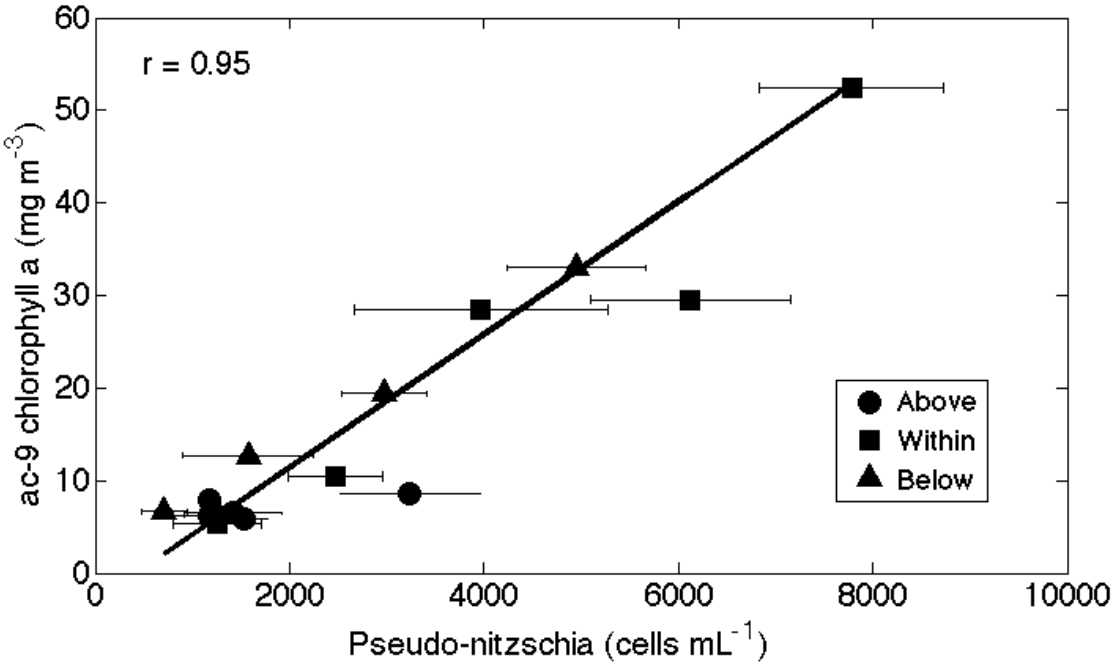

Linear plot of *Pseudo-nitzschia* concentration determined by bottle samples and chlorophyll-*a* concentration measured by the shipboard profiler. Error bars represent the standard deviation about triplicate samples. Samples were grouped by depth: circle = above the layer, square = within the layer and triangle = below the layer. The sample size = 16 & $p < 0.01$.

FIGURE 7. ACROBAT TRANSECT

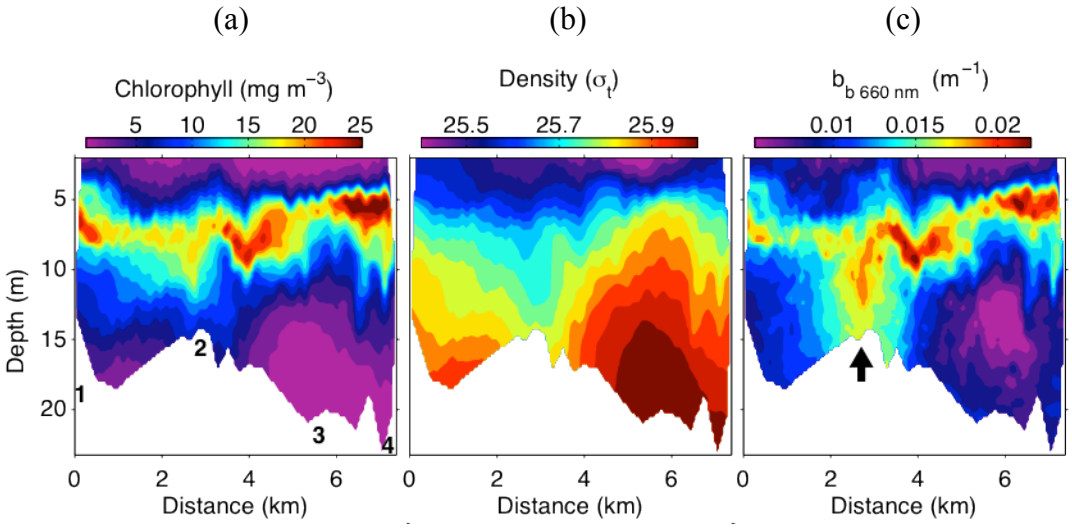

Acrobat transect. Acrobat measurements of: (a) chlorophyll-*a* concentration (mg m^{-3}), (b) density (kg m^{-3}) and (c) optical backscatter at 660 nm (m^{-1}). Numbers 1-4 correspond to the locations on the Acrobat transect from Figure 1. The black arrow indicates where the isopcynals with increased chlorophyll-*a* intersect the seafloor, and increased optical backscatter between the seafloor and the chlorophyll-*a* layer.

APPENDIX A

Appendix A includes data from all discrete water samples from the Lateral Mixing project. Samples 1-3 were the focus of this paper. I have included the depth, date, time, location, TSS, APA, nutrients, chl-*a*, phaeo, DA, phytoplankton counts and flow cytometry counts.

Sample	Depth (m)	Date	Time	Latitude Longitude	TSS ($g\ L^{-1}$)	APA ($nM\text{-}P\ hr^{-1}$)
1	9.8	6/27/10	1500	36.93241 121.92461	0.01428	0.5421
2	18.0	6/27/10	1529	36.93239 121.92461	0.01178	0.2963
3	3	6/27/10	1547	36.93240 121.92461	0.00999	1.0109
4	9.07	6/28/10	1320	36.93241 121.92474	0.01271	0.8066
5	1.72	6/28/10	1420	36.93241 121.92474	0.00756	1.1552
6	3.93	6/30/10	0548	36.93238 121.92529	0.01116	3.3526
7	14.56	6/30/10	0610	36.93236 121.92528	0.01654	1.6329
8	2.32	6/30/10	0629	36.93236 121.92527	0.01071	2.8556
9	6.1	7/2/10	2059	36.93235 121.92496	0.01389	1.0726
10	13	7/2/10	2116	36.932296 121.92496	0.00950	0.9703
11	2.5	7/2/10	2129	36.93235 121.92496	0.00862	2.6202
12	7.4	7/5/10	1308	36^{o}55.946 121^{o}55.487	0.01191	1.5576
13	15.2	7/5/10	1322	36^{o}55.947 121^{o}55.486	0.00733	1.8687
14	4	7/5/10	1336	36^{o}55.947 121^{o}55.486	0.00798	3.2215
15	6	7/9/10	0837	36^{o}55.950 121^{o}55.487	0.00772	2.7924
16	8.9	7/9/10	0853	36^{o}55.952 121^{o}55.486	0.00780	2.9088
17	4	7/9/10	0909	36^{o}55.950 121^{o}55.485	0.00723	2.0119

APPENDIX A (continued)

Sample	Depth (m)	Date	Time	Latitude Longitude	TSS ($g\ L^{-1}$)	APA ($nM\text{-}P\ hr^{-1}$)
18	7.8	10/11/10	1333	36.93259 121.92477	0.01151	4.0620
19	16.4	10/11/10	1349	36.93259 121.92477	0.00764	4.2853
20	2.8	10/11/10	1403	36.93259 121.92477	0.00813	3.9626
21	2.5	10/11/10	1619	36.93259 121.92477	0.01257	3.6024
22	Surf	10/11/10	1809	36.93259 121.92477	0.01968	7.8190
23	Surf	10/13/10	1456	*36.9325 121.9244	0.05362	2.9147
24	Surf	10/15/10	0827	*36.9325 121.9244	0.01256	3.9866
25	7	10/15/10	0856	*36.9325 121.9244	0.01333	2.3221
26	15	10/15/10	0918	*36.9325 121.9244	0.00794	5.2839
27	2	10/15/10	1141	*36.9325 121.9244	0.01494	2.5046
28	10	10/15/10	1225	*36.9325 121.9244	0.00677	3.2794
29	2	10/18/10	1251	*36.9325 121.9244	0.00783	2.5332
30	13	10/18/10	1348	*36.9325 121.9244	0.00770	3.7955
31	5	10/20/10	1252	*36.9325 121.9244	0.00716	2.0761
32	8.3	10/20/10	1309	*36.9325 121.9244	0.00774	4.1142
33	17	10/20/10	1321	*36.9325 121.9244	0.00739	3.4756
34	1	10/20/10	1411	*36.9325 121.9244	0.00872	0.9232

* Latitude and longitude is approximate.

APPENDIX A (continued)

Sample	PO_4 (uM)	$Si(OH)_4$ (uM)	NO_3 (uM)	NO_2 (uM)	NH_4 (uM)	DOC (mg L^{-1})
1	0.34	4.19	4.51	0.11	0.30	2.14
2	1.52	20.38	15.34	0.23	2.52	1.60
3	0.15	1.53	0.54	0.00	0.08	1.40
4	0.38	4.14	5.27	0.11	0.23	3.44
5	0.11	1.87	0.35	0.01	0.06	1.25
6	0.08	1.08	0.23	0.00	0.12	1.35
7	0.41	3.27	3.24	0.08	0.64	1.16
8	0.08	1.09	0.20	0.00	0.06	1.11
9	0.25	1.57	1.45	0.04	0.89	1.49
10	1.05	9.59	7.81	0.17	2.42	1.17
11	0.13	1.73	0.10	0.01	0.06	1.17
12	0.27	1.91	2.29	0.07	0.34	1.04
13	1.58	16.63	12.64	0.23	3.62	0.94
14	0.14	1.24	0.18	0.01	0.08	1.14
15	0.64	5.20	5.31	0.20	0.69	1.76
16	0.84	6.69	7.08	0.24	0.99	1.02
17	0.39	2.49	2.35	0.14	0.33	1.78
18	0.43	21.57	1.93	0.09	0.75	1.01
19	0.84	4.13	5.63	0.19	2.16	0.86
20	0.39	2.03	1.87	0.10	0.53	1.02
21	0.18	2.23	0.48	0.04	0.21	0.99
22	0.14	6.49	0.34	0.02	0.96	1.00
23	0.45	2.56	0.23	0.00	0.23	1.58
24	0.36	2.75	0.23	0.00	0.76	1.19
25	0.35	2.62	0.29	0.00	0.46	1.11
26	0.64	2.75	3.88	0.18	1.48	0.59
27	0.29	2.82	0.27	0.02	0.56	1.19
28	0.43	2.36	1.53	0.09	0.45	0.90
29	0.65	3.41	3.45	0.16	1.32	0.94
30	0.77	4.72	3.79	0.22	2.43	0.94
31	0.63	3.41	2.97	0.17	0.63	0.69
32	0.66	3.54	3.68	0.20	0.35	0.55
33	0.81	5.70	3.72	0.25	2.73	1.04
34	0.58	3.41	2.66	0.16	0.13	0.89

APPENDIX A (continued)

Sample	TP (uM)	TN (uM)	Chl-*a* (ug L^{-1})	Phaeo (ug L^{-1})	dDA (ug L^{-1})	dDA SD	pDA (ng L^{-1})	pDA SD
1	0.68	28.65	34.69	5.74	38.48	-	1715.91	-
2	1.72	26.60	11.68	5.36	2.44	-	1059.29	-
3	0.39	9.86	3.11	3.49	7.12	-	722.98	-
4	0.70	14.55	33.80	4.30	-	-	-	-
5	0.35	9.07	5.35	2.03	-	-	-	-
6	0.30	10.06	10.31	3.66	-	-	-	-
7	0.71	13.10	32.30	4.43	-	-	-	-
8	0.30	9.89	8.54	2.03	-	-	-	-
9	0.36	8.47	19.87	4.68	3.33	1.46	15745.65	1260.96
10	1.23	18.68	17.00	6.18	1.79	1.80	6228.98	204.44
11	0.41	11.15	5.46	2.26	1.20	1.26	2248.21	659.87
12	0.53	10.70	17.21	3.75	6.89	2.83	13587.85	4447.08
13	1.79	25.01	7.02	2.53	4.98	3.28	2617.67	569.76
14	0.43	10.73	4.19	1.50	0.34	0.59	1656.30	408.72
15	0.89	15.09	4.86	1.15	5.16	1.60	806.07	221.36
16	1.06	17.50	5.68	1.60	0.25	0.43	1830.22	750.36
17	0.67	11.70	4.90	0.75	2.21	2.08	2575.35	817.16
18	0.79	22.01	6.04	2.18	2.25	0.36	855.88	290.63
19	1.16	17.94	3.63	0.94	0.00	0.00	1930.70	170.63
20	0.75	12.96	4.88	1.73	0.00	0.00	2646.13	759.96
21	0.44	7.49	3.30	4.80	0.00	0.00	936.44	69.06
22	0.58	9.43	8.88	4.35	0.00	0.00	43.39	6.84
23	1.13	17.16	45.75	77.02	0.00	0.00	0.00	0.00
24	0.74	7.98	17.34	5.09	0.00	0.00	0.00	0.00
25	0.76	8.42	9.29	1.61	0.00	0.00	22.98	6.24
26	0.92	11.63	2.62	2.29	0.00	1.46	15745.65	1260.96
27	0.70	7.60	16.73	5.92	-	-	-	-
28	0.73	7.42	1.50	1.76	-	-	-	-
29	0.99	12.93	1.50	1.42	0.00	0.00	31.38	1.14
30	1.03	13.02	1.05	2.14	0.00	0.00	61.81	8.72
31	1.00	10.26	3.84	3.38	0.00	0.00	2.68	4.65
32	0.97	12.11	3.22	3.06	0.00	0.00	32.12	6.14
33	1.11	15.22	1.24	2.00	0.00	0.00	35.53	9.77
34	0.93	12.50	4.44	1.15	0.00	0.00	4.65	8.06

APPENDIX A (continued)

Sample	Pseudo-nitzschia (cell mL^{-1})	Pseudo-nitzschia SD	Prochloro-coccus L^{-1}	Synechoco-ccus L^{-1}	Photosynthetic eukaryotes L^{-1}	Unpigmented bacteria L^{-1}
1	7783	948.191	12220	1645	3049	6.15E+05
2	1576	674.880	11537	759	1240	4.39E+05
3	1172	107.493	12322	3087	1847	1.54E+06
4	6091	1107.305	19090	987	9678	1.65E+05
5	2429	919.427	13460	2619	1822	8.92E+05
6	2475	487.053	13966	2239	3251	1.22E+06
7	4949	715.551	15067	1290	4719	1.23E+06
8	3237	717.473	14599	2568	3896	2.11E+06
9	6121	1030.637	15952	3732	5123	1.14E+06
10	2975	442.344	13979	2973	3656	9.74E+05
11	1525	249.118	13663	7919	4238	2.17E+06
12	3970	1305.846	15042	5845	3504	1.29E+06
13	1278	355.442	13979	2328	1518	4.00E+05
14	1424	500.688	16876	14460	5035	3.32E+06
15	1258	451.759	15408	26427	4099	6.64E+05
16	712	235.214	13890	21670	8299	9.26E+05
17	1182	420.983	13169	20949	7616	9.03E+05
18	258	-	14738	50577	7704	1.88E+06
19	414	-	12031	47933	10285	3.02E+06
20	247	-	11854	66757	7654	3.36E+06
21	131	-	12853	72425	8957	2.84E+06
22	30	-	11702	70742	5642	3.62E+06
23	5	-	123925	109807	54524	2.02E+06
24	5	-	10411	91211	10715	2.62E+06
25	5	-	13270	87125	14422	3.12E+06
26	106	-	12904	66416	12840	3.70E+06
27	0	-	10247	85670	9792	3.09E+06
28	0	-	8868	58927	7198	2.55E+06
29	10	-	9956	49413	4200	1.35E+06
30	30	-	9172	24909	2808	2.12E+06
31	0	-	8628	72589	11702	1.91E+06
32	5	-	10234	78661	12663	1.61E+06
33	0	-	11246	63506	14384	3.05E+06
34	5	-	11449	76916	9033	1.37E+06

REFERENCES

Alldredge, A.L., Cowles, T.J., MacIntyre, S., Rines, J.E.B., Donaghay, P.L., Greenlaw, C.F., Holliday, D.V., Dekshenieks, M.M., Sullivan, J.M., Zaneveld, J.R.V., 2002. Occurrence and mechanisms of formation of a dramatic thin layer of marine snow in a shallow Pacific fjord. Marine Ecology Progress Series 233, 1-12.

Alldredge, A.L., Crocker, K.M., 1995. Why do sinking mucilage aggregates accumulate in the water column?. The Science of the Total Environment 165, 15-22.

Alldredge, A.L., Gotschalk, C.C., 1989. Direct observations of the mass flocculation of diatom blooms: characteristics, settling velocities and formation of diatom aggregates. Deep-Sea Res. 36, 159–171.

Alldredge, A.L., Gotschalk, C.C., 1990. The relative contribution of marine snow of different origins to biological processes in coastal waters. Cont. Shelf. Res. 10, 41-58.

Alldredge, A.L., Silver, W., 1988. Characteristics, dynamics and significance of marine snow. Prog. Oceanogr. 20, 41–82.

Anderson, C.R., Brzezinski, M.A., Washburn, L., Kudela, R., 2006. Circulation and environmental conditions during a toxigenic Pseudo-nitzschia australis bloom in the Santa Barbara Channel, California. Mar. Ecol. Prog. Ser. 327, 119-133.

Backer, L.C., McGillicuddy, D. J., 2006. Harmful algal blooms at the interface between coastal oceanography and human health. Oceanography 19, 94-106.

Bargu, S., Lefebvre, K., Silver, M.W., 2006. Effect of dissolved domoic acid on the grazing rate of krill Euphausia pacifica. Mar. Ecol. Prog. Ser. 312, 169-175.

Bargu, S., Powell, C.L., Wang, Z., Doucette, G.J., Silver, M.W., 2008. Note on the occurrence of Pseudo-nitzschia australis and domoic acid in squid from Monterey Bay, CA (USA). Harmful Algae 7, 45-51

Bates, S.S., Bird, C.J., de Freitas, A.S.W., Foxall, R., Gilgan, M., Hanic, L.A., Johnson, G.R., McCulloch, A.W., Odense, P., Pocklington, R., Quilliam, M.A., Sim, P.G., Smith, J.C., Subba Rao, D.V., Todd, E.C.D., Walter, J.A., Wright, L.C., 1989. Pennate diatom Nitzschia pungens as the primary source of domoic acid, a toxin in shellfish from eastern Prince Edward Island, Canada. Can. J. Fish. Aquat. Sci. 46, 1203-1215.

Bates, S.S., Freitas, A.S.W., Milley, J.E., Pocklington, R., Quilliam, M.A., Smith, J.C., Worms, J., 1991. Controls of domoic acid production by the diatom Nitzschia pungens f. multiseries in culture: nutrients and irradiance. Can. J. Fish. Aquat. Sci. 48, 1136–1144.

Bronk, D.A., Ward, B.B., 1999. Gross and net nitrogen uptake and DON release in the euphotic zone of Monterey Bay, California. Limnol. Oceanogr. 44, 573-585.

Bronk, D., Glibert, P., Ward, B., 1994. Nitrogen uptake, dissolved organic nitrogen release, and new production. Science 265, 1843-1846.

Brzezinski, M.A., 1985. The Si:C:N ratio of marine diatoms: interspecific variability and the effect of some environmental variables. J. Phyco. 21, 347-357.

Brzezinski, M., Phillips, D., Chavez, F., Friederich, G., Dugdale, R., 1997. Silica production in the Monterey, California, upwelling system. Limnol. Oceanogr. 42(8), 1694-1705.

Buck, K.R., Uttal-Cooke, L., Pilskaln, C.H., Roelke, D.L., Villac, M.C., Fryxell, G.A., Cifuentes, L., Chavez, F.P., 1992. Autecology of the diatom Pseudonitzschia australis, a domoic acid producer, from Monterey Bay, CA. Mar. Ecol. Progr. Ser. 84, 293–302.

Busse, L.B., Venrick, E.L., Antrobus, R., Miller, P.E., Vigilant, V., Silver, M.W., Mengelt, C., Mydlarz, L., Prezelin, B.B., 2006. Domoic acid in phytoplankton and fish in San Diego, CA, USA. Harmful Algae 5, 91-101.

Calleja, G. B., 1984. Microbial Aggregation. CRC Press Inc., Boca Raton.

Caron, D.A., Garneau, M., Seubert, E., Howard, M.D.A., Darjany, L., Schnetzer, A., Cetinic, I., Filteau, G., Lauri, P., Jones, B., Trussell, S., 2010. Harmful algae and their potential impacts on desalination operations off southern California. Water Research 44, 385-416.

Clay, A.S., Medwin. H., 1977. Acoustical oceanography: principles and applications. John Wiley and Sons, New York, NY.

Cowen, R.K., Guigand C.M., 2008. In situ ichthyoplankton imaging system (ISIIS): system design and preliminary results. Limnol. Oceanogr.: Methods 6, 126-132.

Chróst, R.J., 1991. Environmental control of the synthesis and activity of aquatic microbial ectoenzymes. In Chróst, R. J. (ed.), Microbial Enzymes in Aquatic Environments. Springer Verlag, Berlin: 29–59.

Dekshenieks, M.M., Donaghay, P.L., Sullivan, Rines, J.E.B., Osborn, T.R., Twardowski, M.S., 2001. Temporal and spatial occurrence of thin phytoplankton layer in relation to physical processes. Mar. Ecol. Prog. Ser. 223, 61-71.

Dortch, Q., Robichaux, R., Pool, S., Milsted, D., Mire, G., Rabalais, N.N., Soniat, T.M., Fryxell, G.A., Turner, R.E., Parsons, M.L., 1997. Abundance and vertical flux of Pseudo-nitzschia in the northern Gulf of Mexico. Mar. Ecol. Prog. Ser. 146, 249-264.

Doucette G.J., Scholin C.A., Ryan J.P., Tyrrell J.V., Marin R. III, Powell C.L., 2002. Possible influence of Pseudo-nitzschia australis population and toxin dynamics on food web impacts in Monterey Bay, CA, USA. In: 10th International Conference on Harmful Algae. St. Petersburg, FL, 76.

Drapeau, D.T., Dam, H.G., Grenier, G., 1994. An improved flocculator design for use in particle aggregation experiments. Limnol. Oceanogr. 39, 723-729.

Duce, R.A., LaRoche, J., Altieri, K., Arrigo, K.R., Baker, A.R., Capone, D.G., Cornell, S., Dentener, F., Galloway, J., Ganeshram, R.S., Geider, R.J., Jickells, T., Kuypers, M.M., Langlois, R., Liss, P.S., Liu, S.M., Middelburg, J.J., Moore, C.M., Nickovic, S., Oschlies, A., Pedersen, T., Prospero, J., Schlitzer, R., Seitzinger, S., Sorensen, L.L., Uematsu, M., Ulloa, O., Voss, M., Ward, B., Zamora, L., 2008. Impacts of atmospheric anthropogenic nitrogen on the open ocean. Science 320, 893-897.

Dyhrman, S. T., Palenik, B., 1999. Phosphate stress in cultures and field populations of the dinoflagellate Prorocentrum minimum detected by a single-cell alkaline phosphatase assay. Applied and Environmental Microbiology 65, 3205-3212.

Dyhrman, S. T., Ruttenberg, K. C., 2006. Presence and regulation of alkaline phosphatase activity in eukaryotic phytoplankton from the coastal ocean: implications for dissolved organic phosphorus remineralization. Limnol. Oceanogr. 51, 1381-1390.

Fehling, J., Davidson, K., Bolch, C.J., Bates, N.R., 2004. Growth and domoic acid production by Pseudo-nitzschia seriata (Bacillariophyceae) under phosphate and silicate limitation. J. Phycol. 40, 674–683.

Fitzwater, S., Johnson, K., Elrod, V., Ryan, J., Coletti, L., Tanner, S., Gordon, R., Chavez, F., 2003. Iron, nutrient and phytoplankton biomass relationships in upwelled waters of the California coastal system. Cont. Shelf. Res. 23, 1523-1544.

Fritz, L., Quilliam, M.A., Wright, J.L.C., Beale, A.M., Work, T.M., 1992. An outbreak of domoic acid poisoning attributed to the pennate diatom Pseudo-nitzschia australis. J. Phycol. 28, 439– 442.

Fogg, G.E., 1995. Some speculations on the nature of the pelagic mucilage community of the northern Adriatic Sea. The Science of the Total Environment 165, 59-63.

GEOHAB 2008. Global Ecology and Oceanography of Harmful Algal Blooms, GEOHAB Core Research Project: HABs in Stratified Systems. P. Gentien, B. Reguera, H. Yamazaki, L. Fernand, E. Berdalet, R. Raine (Eds.) IOC and SCOR, Paris, France, and Newark, Delaware, USA.

Glibert, P.M., Anderson, D. M., Gentien, P., Granéli, E., Sellner, K.G., 2005. The global phenomena of harmful algal blooms. Oceanography 18, 130-141.

Graham, W.M., 1993. Spatio-temporal scale assessment of an "upwelling Shadow" in northern Monterey Bay, California. Estuaries 16, 83–91.

Graham, W.M., Largier, J.L., 1997. Upwelling shadows as nearshore retention sites: the example of northern Monterey Bay. Cont. Shelf. Res. 17, 509–532.

Gotschalk, C.C., Alldredge, A.L., 1989. Enhanced primary production and nutrient regeneration within aggregated marine diatoms. Marine Biology 103, 119-129.

Hillebrand, H., Sommer, U., 1996. Nitrogenous nutrition of the potentially toxic diatom Pseudonitzschia pungens f. multiseries Hasle. Journal of Plankton Research 18(2), 295-301.

Hoppe, H., 2003. Phosphatase activity in the sea. Hydrobiologia 493, 187-200.

Innamorati, M., 1995. Hyperproduction of mucilages by micro and macro algae in the Tyrrhenian Sea. The Science of the Total Environment 165, 65-81.

Johnson, K.S., Chavez, F.P., Friederich, G.E., 1999. Continental-shelf sediment as primary source of iron for coastal phytoplankton. Nature 398, 697-700.

Karl, D.M., 2000. Phosphorus, the staff of life. Nature, 406, 31-33.

Krishnamurthy, A., Moore, J.K., Zender, C.S., Luo, C., 2007. Effects of atmospheric inorganic nitrogen deposition on ocean biogeochemistry. Journal of Geophysical Research 112, G02019.

Kudela, R., Roberts, A., Armstrong, M., 2004. Laboratory analyses of nutrient stress and toxin production in Pseudo-nitzschia spp. from Monterey Bay, California. In Harmful algae 2002, eds. K.A. Steidenger, J.H. Landsberg, C.R. Tomas, and G.A. Vargo, 136–138. St. Pete Beach, FL: Florida and Wildlife Conservation Commission, Florida Institute of Oceanography, and Intergovernmental Oceanographic Commission of UNESCO.

Kvitek R.G., Goldberg, J.D., Smith, G.J., Doucette, G.J., Silver, M.W., 2008. Domoic acid contamination within eight representative species from the benthic food web of Monterey Bay, California, USA. Mar. Ecol. Prog. Ser. 367, 35-47.

Kwon, H.K., Oh, S.J., Yang, H., 2011. Ecological significance of alkaline phosphatase activity and phosphatase-hydrolyzed phosphorus in the northern part of Gamak Bay, Korea. Marine Pollution Bulletin 62, 2476-2482.

Lefebvre, K.A., Powell, C.L., Busman, M., Doucette, G.J., Moeller, P.D.R., Silver, J.B., Miller, P.E., Hughes, M.P., Singaram,S., Silver, M.W., Tjeerdema, R.S., 1999. Detection of domoic acid in northern anchovies and California sea lions associated with an unusual mortality event. Natural Toxins 7, 85-92.

Lefebvre, K.A., Robertson, A., 2010. Domoic acid and human exposure risks: a review. Toxicon 56, 218-230.

Lefebvre, K.A., Silver, M.W., Coale, S.L., Tjeerdema, R.S., 2002. Domoic acid in planktivorous fish in relation to toxic Pseudo-nitzschia cell densities. Marine Biology 140, 625-631.

Logan, B.E., Alldredge, A.L., 1989. Potential for increased nutrient uptake by flocculating diatoms. Marine Biology 101, 443-450.

Maldonado, M.T., Hughes, M.P., Rue, E.L., Wells, M.L., 2002. The effect of Fe and Cu on growth and domoic acid production by Pseudo-nitzschia multiseries and Pseudo-nitzschia australis. Limnol. Oceanogr. 47, 515–526.

Marchetti, A., Trainer, V. L., Harrison, P. J., 2004 Environmental conditions and phytoplankton dynamics associated with Pseudo-nitzschia abundance and domoic acid in the Juan de Fuca eddy. Mar. Ecol. Prog. Ser. 281, 1-12.

McManus, M.A., Alldredge, A.L., Barnard, A.H., Boss, E., Case, J.F., Cowles, T.J., Donaghay, P.L., Eisner, L.B., Gifford, D.J., Greenlaw, C.F., Herren, C.M., Holliday, D.V., Johnson, D., MacIntyre, S., McGehee, D.M., Osborn, T.R., Perry, M.J., Pieper, R.E., Rines, J.E.B., Smith, D.C., Sullivan, J.M., Talbot, M.K., Twardowski, M.S., Weidemann, A., Zaneveld, J.R., 2003. Characteristics, distribution and persistence of thin layers over a 48 hour period. Mar. Ecol. Prog. Ser. 261: 1–19.

McManus, M.A. Kudela, R.M., Silver, M.W., Steward, G.F., Donaghay, P.L., Sullivan, J.M., 2008. Cryptic blooms: are thin layers the missing connection?. Estuaries and Coasts 31, 396-401.

Mingazzini, M., Thake, B., 1995. Summary and conclusions of the workshop on marine mucilages in the Adriatic Sea and elsewhere. The Science of the Total Environment 165, 9-14.

Mobley, C.D., Sundman, L.K., Boss, E., 2002. Phase function effects on oceanic light fields. Applied optics 41, 1035-1050.

Mos, L., 2001. Domoic acid: a fascinating marine toxin. Environmental Toxicology and Pharmacology 9, 79-85.

Myklestad, S.M., 1995. Release of extracellular products by phytoplankton with special emphasis on polysaccharides. The Science of the Total Environment 165, 155-164.

Olivieri R.A., 1996. Plankton dynamics and the fate of primary production in the coastal upwelling ecosystem of Monterey Bay, California. Ocean Science PhD thesis, University of California, Santa Cruz, California.

Olson, M.B., Lessard, E.J., 2010. The influence of the Pseudo-nitzschia toxin, domoic acid, on microzooplankton grazing and growth: A field and laboratory assessment. Harmful Algae 9, 540-547.

Ou, L., Huang, B., Lin, L., Hong, H., Zhang, F., Chen, Z., 2006. Phosphorus stress of phytoplankton in the Taiwan Strait determined by bulk and single-cell alkaline phosphatase activity assays. Mar. Ecol. Prog. Ser. 327, 95-106.

Pan, Y., Subba Rao, D.V., Mann, K.H., 1996a. Changes in domoic acid production and cellular chemical composition of the toxigenic diatom Pseudo-nitzschia multiseries under phosphate limitation. J. Phycol. 32, 371–381.

Pan, Y., Subba Rao, D.V., Mann, K.H., Brown, R.G., Pocklington, R., 1996b. Effects of silicate limitation on production of domoic acid, a neurotoxin, by the diatom Pseudo-nitzschia multiseries. I. Batch culture studies. Mar. Ecol. Prog. Ser. 131, 225-233.

Pan, Y., Subba Rao, D.V., Mann, K.H., Li, W.K.W., Harrison, W.G., 1996c. Effects of silicate limitation on production of domoic acid, a neurotoxin, by the diatom Pseudo-nitzschia multiseries. II. Continuous culture studies. Mar. Ecol. Prog. Ser. 131, 235-243.

Parsons M, Dortch Q, Turner R., 2002. Sedimentological evidence of an increase in Pseudo-nitzschia (Bacillariophyceae) abundance in response to coastal eutrophication. Limnol. Oceanogr. 47, 551–558.

Passow, U., Alldredge, A.L., 1994. Distribution, size and bacterial colonization of transparent exopolymer particles (TEP) in the ocean. Mar. Ecol. Prog. Ser. 113, 185-198.

Pennington, J., Chavez, F., 2000. Seasonal fluctuations of temperature, salinity, nitrate, chlorophyll and primary production at station H3/M1 over 1989-1996 in Monterey Bay, California. Deep-Sea Research II 47, 947-973.

Pilskaln, C.H., Lehmann, C., Paduan, J.B., Silver, M.W., 1998. Spatial and temporal dynamics in marine aggregate abundance, sinking rate and flux: Monterey Bay, central California. Deep-Sea Research II 45, 1803-1837.

Pilskaln, C., Paduan, J., Chavez, F., Anderson, R., Berelson, W., 1996. Carbon export and regeneration in the coastal upwelling system of Monterey Bay, central California, Journal of Marine Research, 54, 1149-1178.

Rines, J.E.B., Donaghay, P.L., Dekshenieks, M.M., Sullivan, J.M., Twardowski, M.S., 2002. Thin layers and camouflage: hidden Pseudo-nitzschia spp. (Bacillariophyceae) populations in a fjord in the San Juan Islands, Washington, USA. Mar. Ecol. Prog. Ser. 225, 123–137.

Rosenfeld L.K., Schwing F.B., Garfield N., Tracy, D.E., 1994. Bifurcated flow from an upwelling center: a cold water source for Monterey Bay. Cont. Shelf. Res. 14, 931-964.

Ryan, J.P., Chavez, F.P., Bellingham, J.G., 2005. Physical-biological coupling in Monterey Bay, California: topographic influences on phytoplankton ecology. Mar. Ecol. Prog. Ser. 287, 23–32.

Ryan, J.P., Fischer, A.M., Kudela, R.M., Gower, J.F.R., King, S.A., Marin III, R., Chavez, F.P., 2009. Influences of upwelling and downwelling winds on red tide bloom dynamics in Monterey Bay, California. Cont. Shelf. Res.. 29, 785-795.

Rue, E.L., Bruland, K.W., 2001. Domoic acid binds iron and copper: a possible role for the toxin produced by the marine diatom Pseudo-nitzschia. Mar. Chem. 76, 127-134.

Sarthou, G., Timmermans, K.R., Blain, S., Tréguer, P., 2005. Growth physiology and fate of diatoms in the ocean: a review. Journal of Sea Research 53, 25-42.
Schnetzer, A., Miller, P.E., Schaffner, R.A., Stauffer, B.A., Jones, B.H., Weisberg, S.B., DiDiacomo, P.M., Berelson, W.M., Caron, D.A., 2007. Blooms of Pseudo-nitzschia and domoic acid in the San Pedro Channel and Los Angeles harbor areas of the Southern California Bight, 2003-2004. Harmful Algae 6, 372-387.
Sekula-Wood, E., Benitez-Nelson, C. R., Morton, S., Anderson, C, Burrell, C., Thunell, R, 2011. Pseudo-nitzschia and domoic acid fluxes in Santa Barbara Basin (CA) from 1993 to 2008. Harmful Algae 10, 567-575, doi:10.1016/j.hal.2011.04.009.
Sellner, K.G., Doucette, G.J., Kirkpatrick, G.J., 2003. Harmful algal blooms: causes, impacts and detection. J. Ind. Microbiol. Biotechnol. 30, 383-406.
Smetacek, V., 1985. Role of sinking in diatom life-history cycles: ecological, evolutionary and geological significance. Mar. Biol. 84, 239–251.
Smith, J. C., Cormier, R., Worms, J., Bird, C.J., Quilliam, M.A., Pocklington, R., Angus, R., 1990. Toxic blooms of the domoic acid containing diatom Nitzschia pungens in the Cardigan River, Prince Edward Island. In Graneli, E., Sundstrom, B., Edler, L. Anderson, D. M. (eds.), Toxic marine phytoplankton. Elsevier, 227-232.
Subba Rao, D.V., Quillam, M.A., Pocklington, R., 1988. Domoic acid – a neurotoxic amino acid produced by the marine diatom Nitzschia pungens in culture. Can. J. Fish. Aquat. Sci. 45, 2076-2079.
Trainer, V.L., Adams, N.G., Bill, B.D., Stehr, C.M., Wekell, J.C., Moeller, P., Busman, M., Woodruff, D., 2000. Domoic acid production near California coastal upwelling zones, June 1998. Limnol. Oceanogr. 45, 1818-1833.
UNESCO, 1994. Protocols for the Joint Global Ocean Flux Study (JGOFS) Core Measurements IOC Manual and Guides 29.
Valderrama, 1981. The simultaneous analysis of total nitrogen and total phosphorus in natural waters. Mar.Chem. 10, 109-122.
Velo-Suárez, L., González-Gil, S., Gentien, P., Lunven, M., Bechemin, C., Fernand, L., Raine, R., Reguera, B., 2008. Thin layers of Pseudo-nitzschia spp. and the fate of Dinophysis acuminata during an upwelling- downwelling cycle in a Galician Ría. Limnol. Oceanogr. 53, 1816–1834.
Vigilant, V. L., Silver, M. W., 2007. Domoic acid in benthic flatfish on the continental shelf of Monterey Bay, California, USA. Mar. Biol. 151, 2053-2062.
Wang, Z., King, K. L., Ramsdell, J. S., Doucette, G.J., 2007. Determination of domoic acid in seawater and phytoplankton by liquid chromatography- tandem mass spectrometry. Journal of Chromatography A 1163, 169-176.
Warren, J.D., Stanton, T.K., Wiebe, P.H., Seim, H.E. 2003. Inference of biological and physical parameters in an internal wave using multiple-frequency, acoustic-scattering data. ICES Journal of Marine Science, 60, 1033–1046.
White, K., Dugdale, R., 1997. Silicate and nitrate uptake in the Monterey Bay upwelling system, Cont. Shelf. Res., 17, 455-472.
Work, T.M., Barr, B., Beale, A.M., Fritz, L., Quilliam, M.A., Wright, J.L.C., 1993. Epidemiology of domoic acid poison in brown pelicans (Pelecanus occidentalis) and brandt's cormorants (Phalacrocorax penicillatus) in California. Journal of Zoo and Wildlife Medicine 24, 54-62.